IRT EVALUATION OF BOND LAYER THICKNESS FOR CFRP BONDED TO CONCRETE

R L Limerick, P V Mtenga and K S Tawfiq
FAMU-FSU College of Engineering, Civil Engineering Dept., Tallahassee, FL, United States

Abstract: Retrofitting of is a cost effective method of prolonging the useful life of civil structures. Carbon fiber reinforced polymer (CFRP) plates and fabrics are currently being used as external tensile and shear reinforcement. Previous studies have shown that the thickness of the adhesive layer is one of the factors affecting the overall effectiveness of the retrofit. In this paper Nondestructive Evaluation (NDE) method of infrared thermography (IRT) is used to investigate the thickness of the adhesive layer bonding a CFRP plate to a concrete structural element surface. The signal processing technique pulsed phase thermography (PPT) is used to obtain phase images of the specimen. The results from experimental testing and numerical modeling of the thermal show that IRT holds promise for this application. The behavior of the experimental phase values show good agreement with the numerical model over a range of bond layer thicknesses.

Introduction: The current state of the nation's infrastructure has made the development of retrofitting techniques a high priority for civil engineers. Damage such as cracked concrete, insufficient steel reinforcement due to inadequate design, increased loading due to a change in use of a structure or corrosive activity in concrete structural elements compromises the load carrying capacity of these members. The practice of externally bonding steel plates to the tension face of beams with an epoxy adhesive has been very successful except with the obvious drawback of being susceptible to corrosion. Fiber Reinforced Polymer (FRP) plates and fabrics have the advantages of being corrosion resistant. Their high strength to weight ratio increases ease of installation and reduces associated costs. These FRPs can be adhered to concrete to be utilized as flexural reinforcement for concrete members such as beams and slabs. One of the principal failure modes of beams retrofitted for flexure with FRP plates is by peeling off of the plate due to a delamination of the adhesive at the concrete-epoxy interface or peeling off of the concrete cover [1,2]. Furthermore it has also been shown that the thickness of the adhesive layer is one of the factors contributing to this type of failure. Numerous studies have been conducted that show the effectiveness of retrofitting concrete members with FRP plates and the role the adhesive layer plays in the effectiveness of the retrofit system [3,4].

Thus far the application of infrared thermography for the evaluation of FRP retrofitting has been limited mainly to qualitative efforts. Hawkins et al [5] investigated debonding in FRP-wrapped columns that were retrofitted by hand, procured shells and machine wrapping. Mtenga et al [6] identified disbonds in FRP fabric bonded to concrete beams. Miceli used IRT to identify adhesive-starved regions in FRP bridge decks [7]. Starnes [8] investigated the use of infrared thermography to quantitatively size defects in a FRP retrofit. Air voids were placed at different locations between FRP layers and at the concrete interface to simulate defects. In the present study the specimen is a concrete slab with a CFRP plate bonded to its surface with a layer of epoxy. The defect is the non-uniformity of the epoxy thickness. Two aluminum bars with an inclined slot of slope 0.016 along each of their edges were used to create a linearly varying epoxy thickness.

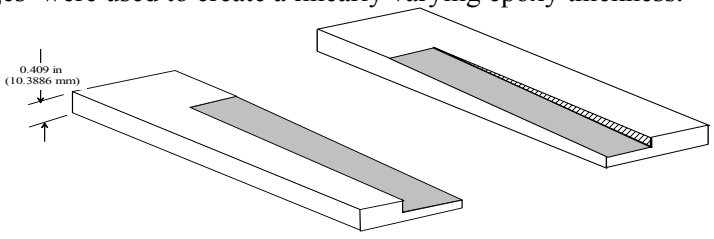

Figure 1: Adhesive forming mold

A plywood box enclosed the specimen on all sides with the top housing six 500 watt halogen lamps and an enclosure for the IR camera in the center. Threaded rods at each corner supported the top of the enclosure so that the height of the camera lens above the CFRP surface could be adjusted.

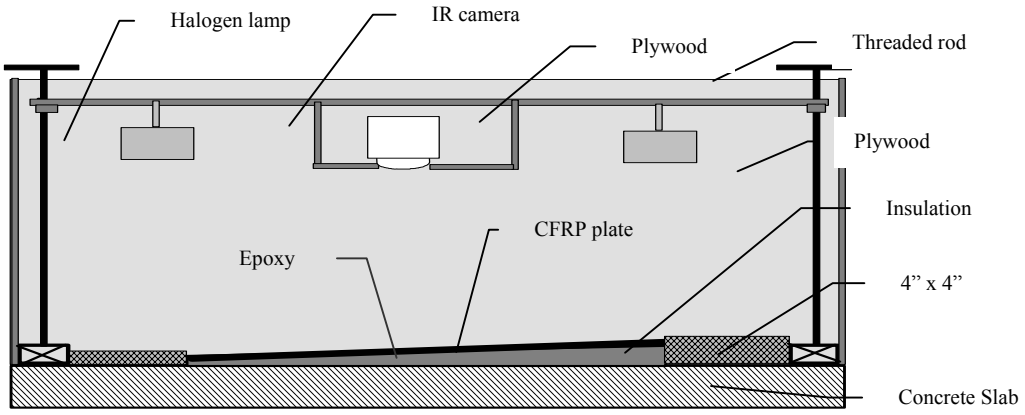

Figure 2: Side elevation of heating setup

The infrared camera used in this study was a Ratheyon® Explor IR. The longitudinal viewing angle of the camera is 26.2°. The vertical distance from the camera lens to the CFRP plate was measured so that the length of the plate in the field of view (FOV) of the camera could be found

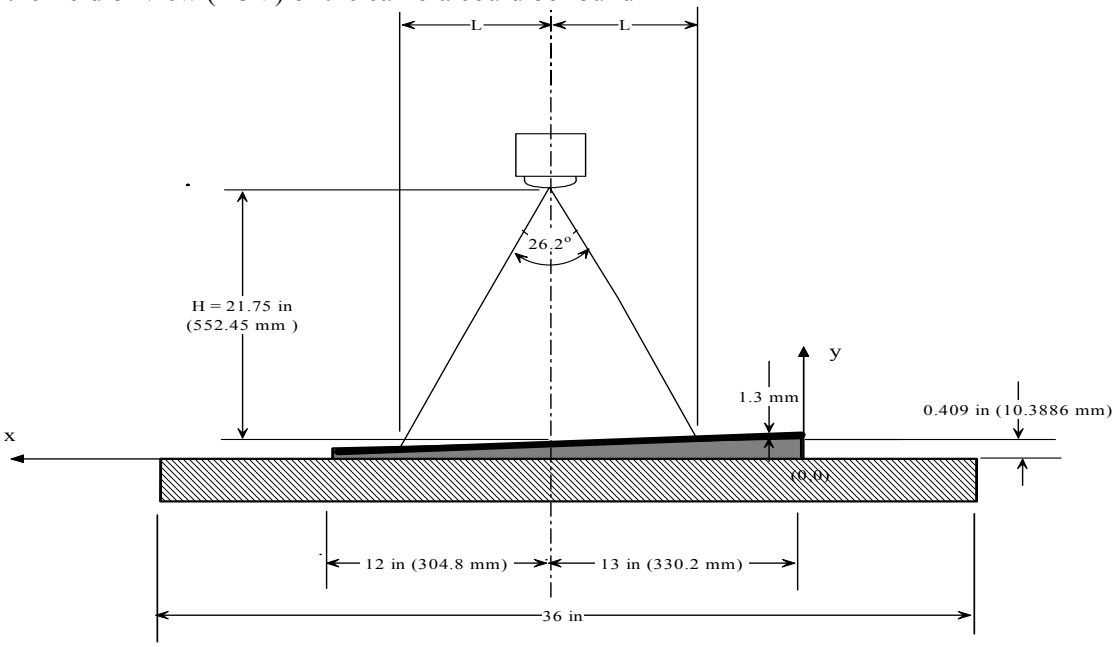

Figure 3: IR camera field of view

The thickness (in millimeters) of the epoxy at any point along the plate is given by

$$y = -0.016x + 10.3886mm \qquad (1)$$

At the right edge of the FOV the epoxy thickness is 7.2 mm. When the thickness of the CFRP plate is added (1.3 mm), the maximum thickness that must be investigated is 8.5 mm. The data is gathered in the form of a digital image 235 pixels in width and 320 pixels in length. The epoxy thickness only varies along the length. The thickness of the epoxy at the center of each pixel needs to be determined. The *x* coordinate for each pixel is found from

$$x_a = \left(x_0 + \frac{p}{2} \right) + a(p) \qquad (2)$$

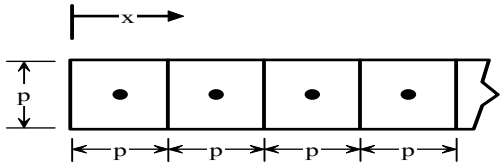

Figure 4: Relationship between pixel width and x-coordinate

Where x_0 = coordinate of the first pixel in the thermogram
a = pixel column number (ranges from 1 to 320)
p = width of a pixel (0.4mm)

The thickness of the adhesive layer at the center of each pixel can now be found by substituting x_a into equation (4) to give

$$y_a = (7.16 - 0.0064a)mm \tag{3}$$

The method of Pulsed phase thermography (PPT) was used in this study. PPT was first introduced by Maldague and Marinetti [9]. In PPT a pulse of heat is applied to the surface of the specimen. The incident heat pulse can be regarded as a thermal wave that is damped as it travels through the specimen. The temporal response of the specimen is then recorded and the discrete Fourier transform (DFT) used to transform the data to the frequency domain. If the temporal evolution of the surface is expressed as a function T (t), the Fourier transform of is given by

$$F(f) = \sum_{n=0}^{N-1} T(n)\, e^{-i\left(\frac{2\pi}{N}\right)fn} \tag{4}$$

Where

N = Number of temperature data points taken over time
f = Frequency index (0, 1, 2, ……., N-1)
n = Temperature data point index (0, 1, 2, ……., N-1)

In the frequency domain the amplitude and phase shift of the transformed data can now be found. The phase shift gives an indication of how the motion of the thermal wave is being impeded by the subsurface. The sampling frequency, f_s, is the inverse of the sampling period, Δt, the time between successive thermograms. The minimum value of Δt is dictated by the capabilities of the infrared camera. There are a multitude of frequencies present in the transformed signal; however, the Shannon sampling theorem dictates that the maximum frequency of interest, f_{max}, must be less than half of f_s. The maximum sampling frequency for the Explor IR is 0.1Hz which leads to f_{max} = 0.05Hz. The frequencies are directly related to the depth to which the thermal wave travels in the specimen. It is necessary to determine the required heating time so that the thermal wave penetrates to the depth of interest. The heat transfer problem in this case is essentially transient heat conduction in a semi-infinite multilayer slab. The solution to this heat conduction problem is complex. A single-layer semi-infinite slab model was used only for the purpose of estimating the required heating time to penetrate the thickest region of the epoxy layer.

The governing equation for 1-D heat conduction is expressed as the following partial differential equation (PDE)

$$\frac{\partial^2 T}{\partial y^2} = \frac{1}{\alpha}\frac{\partial T}{\partial t} \tag{5}$$

$$\alpha = \frac{k}{\rho C_p} \tag{6}$$

k = thermal conductivity (W/m ^oC)
ρ = density (kg/m^3)
C_p = heat capacity (J/kg ^oC)

Table 1: Material properties of specimen

	Concrete	Epoxy	FRP Plate
Density (kg/m^3)	2400	1300	1600
Heat Capacity (J/kg ^{o}C)	800	1700	1200
Conductivity (W/m ^{o}C)	1	0.2	K_X = K_Z= 7 K_Y = 0.8
Thermal Diffusivity (m^2/s) x 10^{-6}	0.52	0.09	0.42

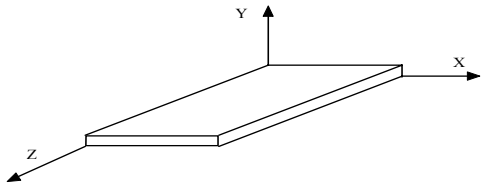

Figure 5: Coordinate axes of specimen

For a semi-infinite slab we have the following boundary conditions

$$Q = -k\frac{\partial T}{\partial y} \text{ at } y = 0 \tag{7}$$

and

$$T = 0 \text{ at } y = \infty \tag{8}$$

Where Q = Heat flux (W/m^2)
T =Temperature(^{o}C)
y = distance in the direction of heat flow (m)

The solution of (5) is

$$T(y,t) = T_i + Q\frac{2\sqrt{\frac{\alpha t}{\pi}}}{k}\exp\left(\frac{-y^2}{4\alpha t}\right) - Q\frac{y}{k}erfc\left(\frac{y}{\sqrt{4\alpha t}}\right) \tag{9}$$

If μ is defined as the depth to which heat travels into the medium over time then $\mu = y$ when $\frac{dT}{dy} = 0$. Taking the derivative of (9) gives

$$\frac{dT}{dy} = -\frac{Q}{k}erfc\left(\frac{y}{\sqrt{4\alpha t}}\right) \tag{10}$$

Setting (10) equal to zero gives

$$erfc\left(\frac{y}{\sqrt{4\alpha t}}\right) = 0 \tag{11}$$

Now $erfc(\infty) = 0$ so $\frac{y}{\sqrt{4\alpha t}} = \infty$. This implies that some miniscule fraction of the applied heat will reach $y = \infty$. This is not a feasible answer to the problem. y = *erfc(x)* decreases quite rapidly. The energy of the thermal wave is heavily damped as it travels through the media. At larger values of x the energy of the wave may be too low to give any useful information, At x = 1, erfc(x) is approximately 16% of its original value. If we take erfc(x)

= 1, then $\frac{\mu}{\sqrt{4\alpha t}} = 1$. This leads to the following expression for the thermal diffusion length of a thermal wave in a semi-infinite medium

$$\mu = 2\sqrt{\alpha t} \qquad (12)$$

A rough estimate of the heating time was made by using (12). The thermal properties of the epoxy were used to estimate maximum heating time. The epoxy has a lower diffusivity than the CFRP plate so this estimate is conservative. For a heating time of five minutes, the heat will propagate into the approximately 10 mm. A theoretical analysis was carried out using a commercial finite element (FE) software package, ANSYS®, to simulate the heat conduction process through the specimen for both heating and cooling. The heat flux at the slab surface heat flux was 968 W/m^2.

Results: The raw data for each of the three test cases were first averaged and then altered to start at 25^{o}C.(the initial temperature in the FE model). The difference between the averaged data and 25^{o}C was typically less than two degrees. The heating and cooling sequences were then fitted using six and seven degree polynomials respectively. The temperature-time profiles presented are for a single pixel located on the longitudinal centerline of the plate at an epoxy thickness of 7mm (Figure **6**). The experimental results for the heating sequence shows good agreement with the theoretical data. After approximately three minutes of heating the experimental data deviates slightly from the theoretical data and the maximum experimental temperature is less than that predicted by theory. This indicates that the incident heat energy is being diverted. This is due to the fact that there is a two dimensional flow of heat in the uneven adhesive layer. The DFT with length N, is applied to the temporal data. For the heating sequence, the phase vs. frequency plots of a pixel show good agreement between experiment and theory at higher frequencies (Figure 7**)**

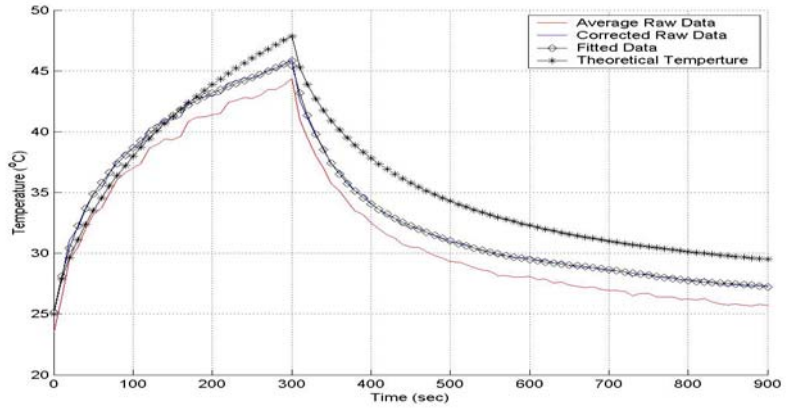

Figure 6: Temperature profiles

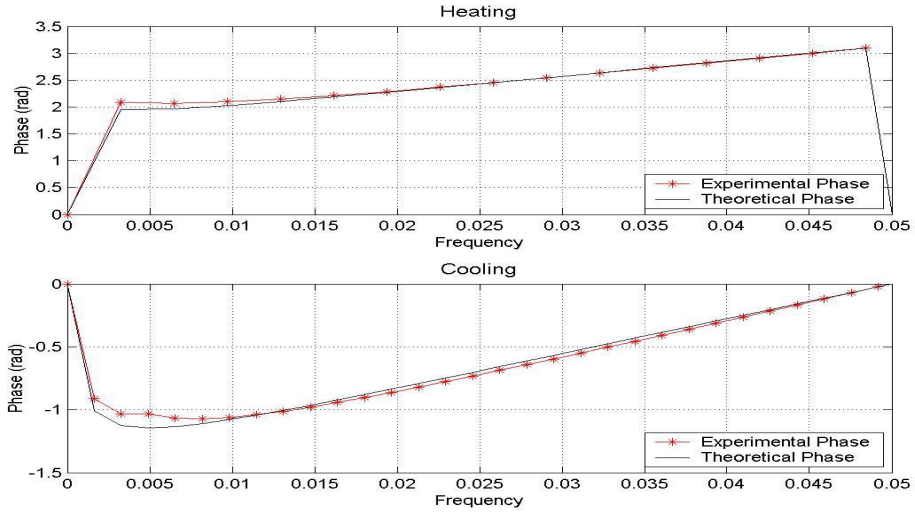

Figure 7: Phase vs. Frequency for Heating and Cooling Sequence (N = No. of data points)

At lower frequencies there is some deviation. Lower frequencies give an indication of the phase of the thermal wave at deeper depths. The discrepancies between the two plots are due to the FE model's assumption of perfect contact between the surfaces and non uniform heat conduction due to the plate thermal properties and the uneven epoxy thickness. The cooling sequence reiterates the fact of imperfect contact resistance but more importantly highlights abrupt changes in the phase at low frequencies. This is due to the thermal wave interacting with the plate-epoxy interface and the concrete-epoxy interface. The cooling phase has more information to offer in this respect since the thermal wave returning from the subsurface has less interference from the anisotropic thermal properties of the CFRP plate.

A plot of theoretical maximum phase against epoxy shows that as the epoxy thickness increases the ability to discern between different thicknesses is diminished **(Figure 8)**. Plots of maximum experimental phase where the DFT length is equal to the number of data points are very noisy and do not show a noticeable trend. Increasing the length of the DFT helped to improve the phase images **(Figure 9)**.

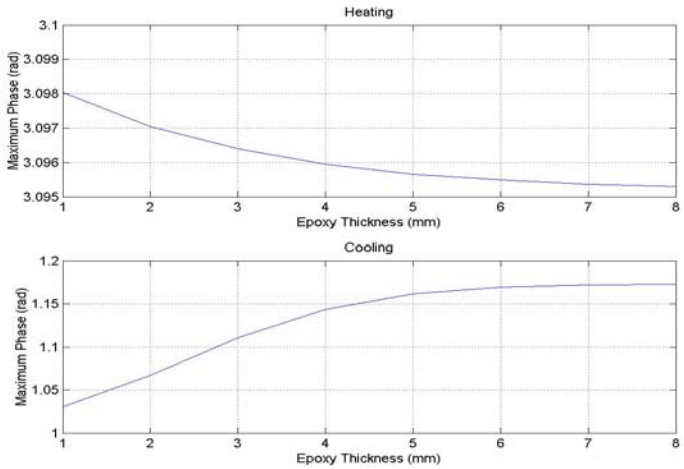

Figure 8: Phase vs Epoxy Thickness (N = No. of data points)

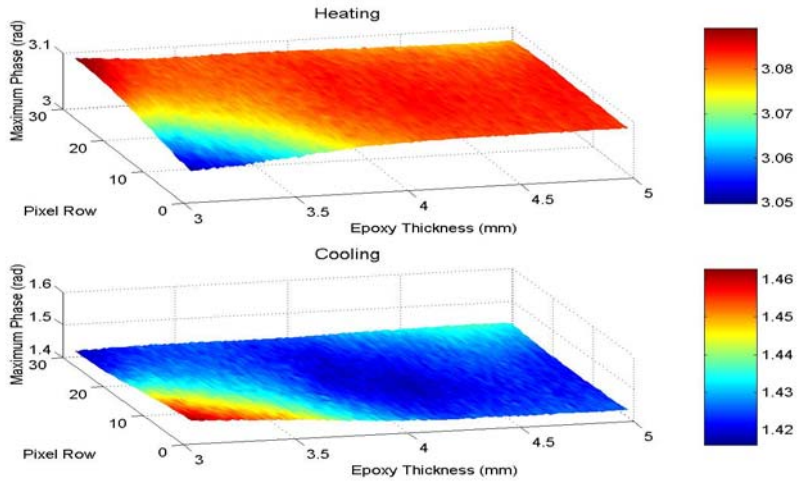

Figure 9: Maximum phase surface – (N= 122)

A DFT length of 122 was chosen for further analysis of maximum phase images. The phase-frequency plots do not offer any additional information for the increased length of the DFT. The theoretical plot of maximum phase versus epoxy thickness for the heating sequence shows the same reduced ability to discern between different thicknesses in thicker epoxy regions **(Figure 10)**. For the cooling sequence it can now be seen that any thickness over 5mm cannot be detected. This turning point of 5mm does not depend on the length of the DFT. The experimental data also suggests that phase values are constant after an epoxy thickness of about 4mm. Information on the heating phase is available from time = 0 up to five minutes. Visual inspection of this phase images shows a similar amount of information to phase images at later heating times. It is therefore possible to get information in a much shorter time provided that the sampling rate is sufficient to adequately capture the thermal process.

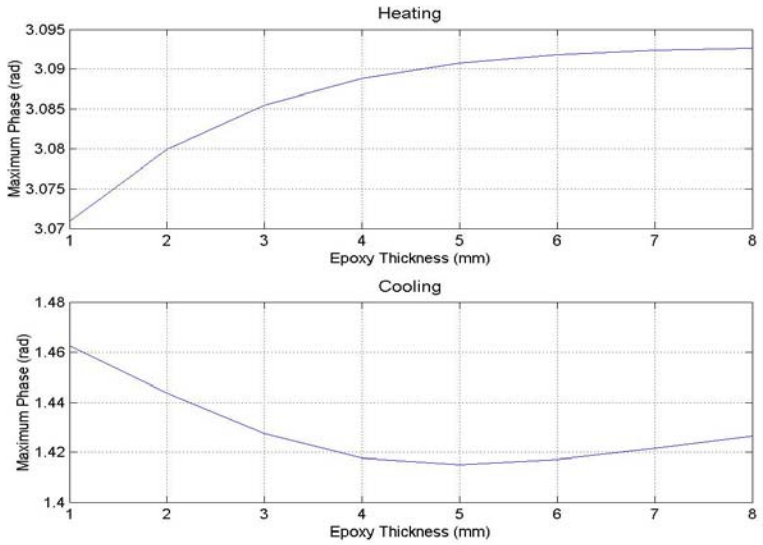

Figure 10: Phase vs Epoxy Thickness (N = 122)

Conclusion: The maximum phase values for the cooling sequence were found to be smaller than the heating sequence because the attenuation of the propagated thermal wave through the specimen. The cooling phase showed a better distinction of the layering system of the cross section of the samples. From the FE model, thicknesses up to 5mm were discernable, but the experimental data could only discern thicknesses up to 4mm. In some cases, the influence of the multidimensional heat flow, uneven heating, and inaccuracies during pouring of the epoxy resulted in difference between experimental and theoretical values. Infrared thermography can be used to provide reasonable estimates of bond layer thickness for pultruded FRP plates given the thermal properties and densities of the FRP and bond

material. The maximum discernable thickness was dependent on these properties. Measurements under field conditions should be collected in a manner that would negate the effects of convection on the induced temperature.

Acknoweledgments: This work was supported from a grant from the Florida State University Research Foundation. The opinion expressed in paper is solely those of the authors and does not reflect the opinion of the Foundation. This support is appreciated.

Refrences:

[1] Saadatmanesh, H.; Ehasani, R.M. RC Beams Strengthened with GFRP Plates II: Experimental Study. ASCE Journal of Structural Engineering, Vol. 117, No. 11, Nov. 1991.

[2] An, W.; Saadatmanesh, H.; Ehasani, R. M. RC Beams Strengthened with FRP Plates II: Analysis and Parametric Study. ASCE Journal of Structural Engineering, Vol. 117, No. 11, Nov. 1991.

[3] Lau K T, Dutta P K, Zhou L M, Hui D, 'Mechanics of bonds in an FRP bonded concrete beam,' Coposites. Vol 32 (2001) 491-502

[4] Smith, S.T.; Teng, J.G. Interfacial Stresses in plated beams. Engineering Structures. Vol. 23 2001 pp857-871

[5] Hawkins, G F, Johnson, E, Nokes J, Typical Manufacturing Flaws in FRP Retrofit Applications. National Institute of Standards and Technology Workshop On Standards Development for the Use of Fiber Reinforced Polymers for the Rehabilitation of Concrete and Masonry Structures Proceedings. 1998 3-97 – 3-101

[6] Mtenga P V, Parzych J, Limerick R L, 'Quality Assurance of FRP Retrofit using Infrared Thermography,' Proceedings of ASCE Structures Congress, Washington DC 2001.

[7] Starnes, M A, 'Development of Technical Bases for Using Infrared Thermography for Nondestructive Evaluation of Fiber Reinforced Polymer Composites Bonded to Concrete', Massachusetts Institute of Technology, 2002

[7] Miceli, M, 'Assessment of Infrared Thermography as NDE Method for Investigation of FRP Bridge Decks', Virginia Polytechnic and State University, 2000

[9] Maldague, X. and Marinetti, S. 'Pulse Phase Infrared Thermography' Journal of Applied Physics. Vol. 79(5) (March 1996) 2694-2698

[10] Maldague, X., Largouet, Y. and Couturier, J.S. 'Study of defect depth using neural networks in pulsed phase thermography: Modelling, noise, experiments' Revue Générale de Thermique, Volume 37(8) September 1998 704-717

[11] Limerick R 'Nondestructive determination of adhesive bond thickness using Infrared Thermography', Florida Agricultural and Mechanical University, 2003